e-J. Surf. Sci. Nanotech. Vol. 4 (2006) 394-400 Conference -ALC05-

Particle Scattering off Surfaces: Application in Space Science*

Peter Wurz,† Jürgen Scheer, and Martin Wieser‡
Physics Institute, University of Bern, CH-3012 Bern, Switzerland
(Received 24 October 2005; Accepted 15 February 2006; Published 16 April 2006)

In many applications of remote sensing of plasma populations in space science a high detection efficiency of energetic neutral atoms (ENAs) is necessary because the sources of these ENAs are very faint. In the recent years surface science processes occurring during particle scattering off specialized surfaces have been successfully used to detect these ENAs with high efficiency. The relevant processes are kinetic secondary electron emission and surface ionization. When secondary electron emission is used an ENA hits a so-called start surface where it releases a secondary electron, which initiates the measurement sequence. Being scattered off the start surface, the ENA continues its flight until it is absorbed at the stop detector. The time difference between the release of the secondary electron and the detection of the particle at the stop detector is measured and with the path length the velocity of the particle is obtained. Surface ionization, i.e., the formation of negative ions, is the well-known charge transfer process where an atom receives an electron from the scattering surface during the scattering process. In modern space science applications mostly insulating surfaces are used as conversion surfaces since these do not need any preparation in space to be operable and at the same time have very stable performance over years. In this paper we will show the current status of surface-science-based detection technology that is used in present space missions of the European Space Agency (ESA) and the U.S. American space agency (NASA). [DOI: 10.1380/ejssnt.2006.394]

Keywords: Secondary electron emission measurements; Low energy ion scattering; Electron emission; Ion-solid interactions; Insulating surfaces

I. INTRODUCTION

The detection of energetic neutral atoms (ENAs) in space allows for remote sensing observations of space plasma populations [1]. These populations can be the various plasma entities of the terrestrial magnetosphere, the magnetospheres of other planets, and even the plasma surrounding our solar system beyond the termination shock. With an instrument, which not only records the mass and the energy of a registered particle, but also the arrival direction in one or two dimensions 2D maps of such plasma distributions are obtained, which are line-of-sight integrals of 3D plasma distributions. To obtain the original 3D distribution one needs to interpret these data with 3D models of the plasma population under investigation. Remote sensing via ENA detection marked a major improvement to the *in situ* plasma measurements with ion detection instruments and has been recently reviewed [1]. For *in situ* plasma measurements the spacecraft flew through the plasma population and the plasma phase space density was recorded along the spacecraft trajectory. After several orbits around a planet a reasonable picture of the plasma distribution began to emerge from the recorded data. However, *in situ* measurements always suffered from the problem to distinguish between spatial and temporal variations of the investigated plasma population.

A particularly difficult energy range for ENA detection is that of low-energy neutral atoms (LENAs) with energies ranging from 10 eV to a few keV, which we will discuss in this paper. Nevertheless, this is a very interesting and important energy range to observe since it is the first step when the thermal plasma (e.g. ionospheric plasma at sub-eV energies) is energized in a planetary magnetosphere or some other space plasma system. The first ENA instrument operating in this low energy range is the LENA instrument on the IMAGE mission of NASA [2, 3] with the IMAGE mission being dedicated to the investigation of the terrestrial magnetosphere by imaging instrumentation for particles and photons [4]. The IMAGE spacecraft was launched on 25 March 2000 and is still in operation. Presently, the ASPERA-3 instrument on the Mars Express spacecraft of the European Space Agency (ESA) has a low-energy neutral particle detector in use to investigate the plasma populations around Mars [5]. An identical instrument, the ASPERA-4 instrument, will be used at Venus [6]. Neutral particle imaging of LENAs is foreseen for future space missions as close as our Moon [7] and as far away as planet Mercury [8].

All these instruments are basically single-particle instruments, that is, each registered particle is analysed individually, for its mass, energy, and arrival direction. In the above-mentioned applications surface science effects are used in various ways for the detection of the particles. Unfortunately, the simple detection method used at higher energies of letting these energetic atoms pass a thin carbon foil fails to work at energies lower than about 1 keV/nuc. The surface science effects are used instead for detection, which are secondary electron emission and surface ionisation (to form negative ions). In both cases, the incident neutral atom is scattered from a suitable surface that has been optimised either for high secondary electron yield or for efficient ionisation. Of course, these scattering surfaces have to be as flat as possible (preferably atomically flat because atoms scattering off the surface encounter roughness at the atomic scale) so that angular and energy scatter is low enough not to alter the atoms properties (energy, flight direction) too much for subsequent analysis. In our applications we not only want to

*This paper was presented at 5th International Symposium on Atomic Level Characterizations for New Materials and Devices (ALC05), Hawaii, USA, 4-9 December, 2005.
†Corresponding author: peter.wurz@phim.unibe.ch
‡Present address: Swedish Institute of Space Physics (IRF), SE-981 28 Kiruna, Sweden

measure the particle flux and identify the species but also recover their arrival direction and their incident energy, thus the scattering event at the surface has to be optimized and the surfaces we use have to be atomically flat and have electronic properties that optimize secondary electron emission or surface ionization.

To detect single neutral atoms in the presence of several intense background sources (UV photons, plasma ions and electrons, high energy particles,) a coincidence technique is often employed [1], which means that for the successful detection of a particle it has to trigger at least two detectors in proper succession and time difference. Typically a time-of-flight (TOF) measurement is performed and with the known distance from the start detector (the first detector) to the stop detector (the second detector) the velocity of the atom is derived. With an additional measurement the mass of the particle can be inferred. This detection technique will be discussed in Section II below. If one wants to characterise the ENA in more detail it has to be ionised so that an ion-optical analysis can be performed. This technique will be discussed in Section III below.

II. DETECTION VIA SECONDARY ELECTRONS

When an energetic atom or ion hits a solid surface electrons are released, which is called kinetic electron emission (KEE). In the simplest form the KEE yield, γ_{KEE}, is considered to be proportional to the electronic stopping power of the impacting particle on the target surface [10],

$$\gamma_{KEE} = \frac{\Lambda}{\cos\varphi} S_e = \frac{\Lambda}{\cos\varphi} k_e \sqrt{E}, \qquad (1)$$

where Λ is the proportionality factor and φ is the angle of impact measured from the surface normal. The electronic stopping power, S_e, is proportional to the velocity of the impacting particle, i.e., $S_e \propto \sqrt{E}$ in the Lindhard-Scharff velocity regime where $v \leq Z^{2/3} v_n$ with $v_n = \alpha c \approx 2.18 \times 10^6$ m/s [11].

KEE during particle scattering from surfaces is the principle of detection of the Neutral Particle Detector (NPD) of the ASPERA-3 instrument on the Mars Express mission of ESA [5]. As start surface a multi-layer coating on a highly polished tungsten substrate is used in NPD. Incoming particles impact on the start surface at shallow angle (about 75° from surface normal) and are forward scattered into the NPD sensor. During the interaction of the ENA with the start surface one or more electrons are released that are registered with a MCP detector and serve as start pulse for the TOF measurement. After a flight path of about 5 cm the ENA hits a stop detector, which is MgO coated graphite. Again, upon particle impact, electrons are released, registered with a MCP detector and used as stop pulse for the TOF measurement. The choice of start surface was driven by the need for good particle reflection properties, e.g. a very flat surface and high-Z material, and good suppression of UV light against forward scattering into the instrument. The latter is achieved by the multi-layer coating composed of a thin layer of Cr_2O_3 covered by a thicker layer of MgF_2 and topped with a thin layer of WO_2. The multi-layer coating was optimized to absorb UV photons at the Lyman-α wavelength. The stop detector had to have a high KEE yield but should not be sensitive to visible and UV light. MgO has a high, perhaps the highest, KEE yield of all insulators [12]. In addition, MgO is an insulator with a band gap of 7.8 eV [13], thus photons with wavelengths greater than about 159 nm will not cause the release of photoelectrons. The graphite substrate of the stop detector serves to absorb all the photons transmitted through the MgO coating rather than reflecting them back into the sensor, where they would cause background on the stop detectors.

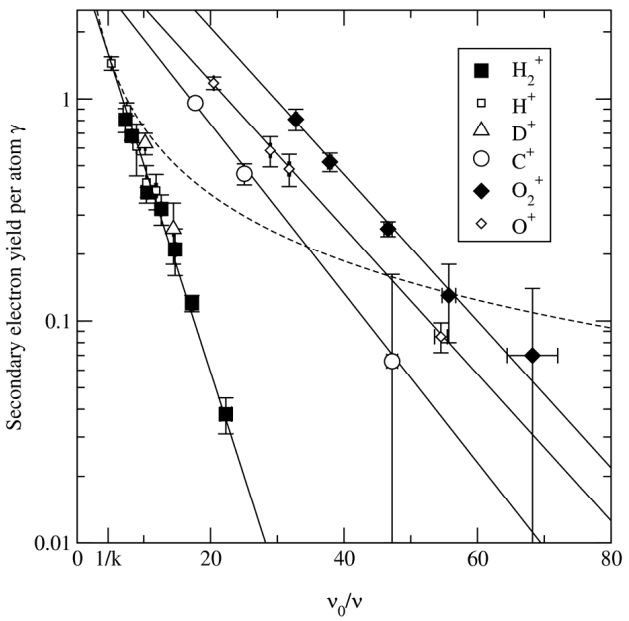

FIG. 1: Secondary electron yield for various primary particles impinging at 60° to the surface normal [9]. Straight lines are fits using Eq. (2) with $\gamma_0 = 4.35$ for H, D, and H_2, $\gamma_0 = 4.46$ for C, $\gamma_0 = 5.51$ for O, and $\gamma_0 = 9.56$ for O_2. The dashed line shows the linear approximation corresponding to Eq. (1): $\gamma = (\Lambda/\cos\alpha) k_e v$.

Since there are several, at times conflicting, requirements for these surfaces there is still research going on to find the perfect surface for applications on a spacecraft. Figure 1 shows the KEE yield measurements of chemical-vapour deposited diamond on silicon using several primary ions in the energy range from 30 eV to 3 keV [9]. Although we do not observe a threshold energy for the KEE, the useful energy range extends down to energies of about 100 eV or less depending on species for our applications. From Fig. 1 one immediately recognises that the simple formula for the secondary electron yield given in Eq. (1) overestimates the KEE yield at low particle energies. A more accurate formula at low particle energies is

$$\gamma_{KEE} = \frac{\gamma_0}{\cos\varphi} \exp\left(\frac{-v_0 k}{v\sqrt{Z_1}}\right), \qquad (2)$$

where v is the particle velocity, k is a projectile species independent constant ($k = 0.215$), Z_1 the atomic number of the projectile, and γ_0 is the asymptotic electron yield for

$v \to \infty$, which is an experimentally determined constant for each species and surface [9]. Again we assume a cosine angular dependence, although at low particle energies this is a simplification [15]. A dependence of $\gamma \propto e^{-A/v_\perp}$ with A being a constant and $v_\perp$ the velocity of the projectile perpendicular to the surface was also reported before where a surface electron-hole pair excitation mechanism was identified for the emission of secondary electrons from slow Li^+ ions impinging on aluminium [16]; however, no projectile-type dependence was reported there. Surface-assisted kinetic electron emission is identified as a dominant mechanism for electron emission for data reported for C^+, N^+, and O^+ impinging on a polycrystalline gold surface [17, 18]. These data are also fitted well with the function shown in Eq. (2). Note that our data do not show a threshold velocity for secondary electron emission similar to earlier findings [19]. When Eq. (2) is expanded at the velocity $v = v_0 k$ we get the power series

$$\begin{aligned} \gamma_{KEE} &\approx \frac{\gamma_0}{\cos\varphi}\left\{\left(1-\frac{1}{\sqrt{Z_1}}\right)e^{-\sqrt{1/Z}} + \frac{v}{v_0 k}\frac{1}{\sqrt{Z_1}}e^{-\sqrt{1/Z}} + ...\right\} \\ &= a + \frac{v}{v_0}b + ... \end{aligned} \tag{3}$$

which simplifies to the well-know linear velocity dependence of the KEE yield ($\gamma \propto v$, as given in Eq. (1)) and a even vanishes for hydrogen.

Because the KEE yield of MgO is very high the number of electrons emitted can be used to infer the mass of the incident particle. Once the velocity of the registered particle is known from the TOF measurement one can use the mass dependence in the proportionality factor k_e in Eq. (1) [11] to infer the mass of the particle. This effect is used for the distinction between hydrogen and oxygen atoms, the two main constituents in the Mars environment, in the NPD sensor of ASPERA-3 [5]. Figure 3 shows a histogram of a Monte-Carlo (MC) simulation of the KEE yields (the pulse height distribution, PHA) for a mixture of 80% hydrogen and 20% oxygen impinging on a MgO surface for the energy range of the NPD detector. The MC simulation includes the measured KEE yields, the resolution of the velocity measurement of the NPD sensor, and applies Poisson statistics for the number of emitted electrons. One can see from Fig. 3 that the distinction between H and O can easily be made on a statistical basis.

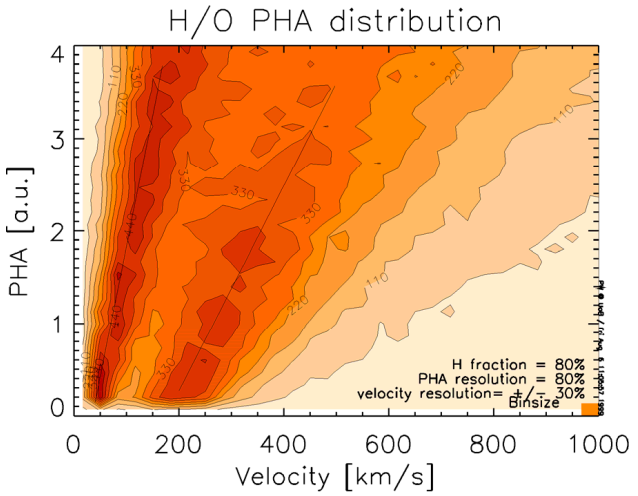

FIG. 2: Monte-Carlo simulation of the pulse height distribution (PHA) of the KEE for hydrogen and oxygen impacting on a MgO surface.

III. DETECTION VIA SURFACE IONIZATION

To extend the useful energy range for ENA measurements down to 10 eV and to improve on the analysis of the registered ENAs one has to ionise the ENAs before further analysis in the instrument. Once an ENA is ionised one can use the established ion-optical techniques for energy and mass analysis of the ion. Surface ionisation was identified as the only viable ionisation technique giving acceptable ionisation yields within the very limited availability of resources on a spacecraft, which are power, mass, volume, and some others [1, 20]. With surface ionisation we mean the transfer of an electron from the surface to the projectile during the scattering event, i.e., forming a negative ion, which only works for elements that have a stable negative ion [21]. Our preference for negative ions is because the ionisation yield is significantly higher than for positive ions at lower projectile energies [22], at least for H and O, which are of highest importance in our research.

Since the early 1980s, surface ionisation has been studied extensively for potential application in fusion plasma research. With this technique, ionisation efficiencies of up to 67% in the energy range from several eV to about 1 keV have been achieved [23–25], using low work function (WF) surfaces for converting neutral particles or positive ions into negative ions. In these applications of surface ionization a metal surface has been used, where the work function of the surface was significantly reduced by the application of a monolayer or less of an alkali metal [26] or an alkaline-earth metal [27]. The application of this overlayer of metal usually involves a dispenser, which releases defined quantities of the metal upon heating, to coat the metal substrate. Since the alkali metal and to a lesser degree the alkaline-earth metal surface are chemically very sensitive, they degrade even in good vacuum after some time, and regeneration of the converter surface at regular intervals is necessary for long-term operation. This regeneration of the converter surface involves heating of the

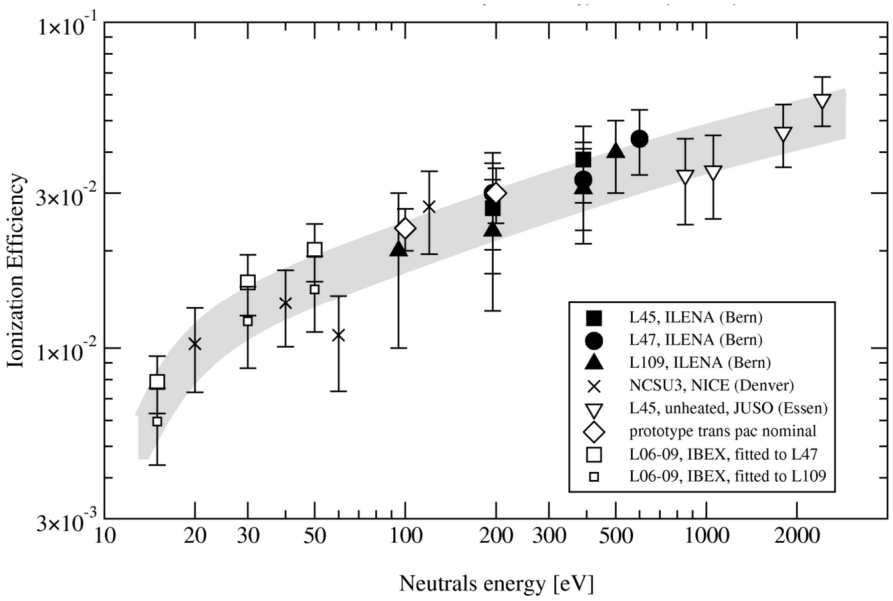

FIG. 3: Efficiency for creating negative hydrogen ions upon scattering from several synthetic diamond coatings on silicon [14]. Measurements have been performed at different laboratories with different experimental setups.

surface to substantial temperatures to evaporate the adsorbates, and the alkali or alkaline-earth metal overlayer. Then, one proceeds with the application of a fresh alkali or alkaline-earth metal layer. In addition to heating the surface to substantial temperatures, the handling of a dispenser introduces some complexity, as well as monitoring the WF of the surface [28].

The first instrument to use surface ionisation in space is the LENA instrument [2, 29], which is successfully operating since the launch of the IMAGE spacecraft on 25 March 2000 [3]. The LENA instrument uses highly polished tungsten as conversion surfaces. Originally, it was intended that these surfaces will be covered with a cesium coating applied in space but it turned out that this was technically not feasible in a space application. However, reasonably high ionisation yields are obtained because of the oxidation of the tungsten surface. This oxidation is routinely replenished because the IMAGE spacecraft dives regularly into the terrestrial exosphere during its 8 hour orbit where there is atomic oxygen in abundance.

Given the complexity of using metallic surfaces with lowered work function as conversion surfaces, we were investigating alternatives, where the regeneration of the surface would be easier or not necessary at all. In addition, these surfaces should be stable in air to simplify operations during spacecraft launch. The search for alternative conversion surface materials was mostly focused on insulators, since we conjectured that surfaces with a high KEE would also work well for surface ionisation. In addition, insulator surfaces often are chemically stable in air even at modest humidity.

We successfully investigated diamond coatings on silicon wafers [30], natural diamond [31], and tetrahedral amorphous carbon coatings on silicon wafers [32], which all turned out to be possible candidates for an application in space. Furthermore, we investigated aluminum nitride coatings [33] and barium zirconate coatings [34], which worked well but are difficult to obtain in good quality at larger quantities. Magnesium oxide was also investigated [35, 36], but the ionisation yield is a little bit low and MgO is hygroscopic. Lithium fluoride surfaces were also investigated because at higher projectile energies negative ion yields of up to 70% for oxygen upon scattering from LiF were reported [37]. However, at the projectile energies of interest for us the ionisation yields were too low [38]. In addition, LiF is chemically not a very stable surface in air.

TABLE I: Fit parameters for Eq. (4) using the three data sets from Figs. 3 to 5. Note that the value for H scattered off diamond coatings is not constrained very well.

	H scattered off diamond coatings	O scattered off diamond coatings	O scattered off MgO
η_0^-	0.135	0.135	0.085
E_0 (eV)	20	118	108
a	0.31	0.4	0.4
b	1.5	2.44	2.44

Figures 3 to 5 show ionisation yields, which is the fraction of negative ions in the scattered particle flux, for hydrogen and oxygen over the full energy range of interest for two currently investigated surfaces, tetrahedral amorphous carbon and magnesium oxide. Quantitative measurements using neutral atoms are difficult and even more so at lower energies. For that reason measurements performed at different facilities with different experimental approaches are given, which agree with each other within the experimental error. The facilities are the ILENA experiment at the University of Bern [14, 30], the JUSO facility at the University of Osnabrück [34, 39], measurements using the NICE prototype at the calibration of the University of Bern and University of Denver [22], and

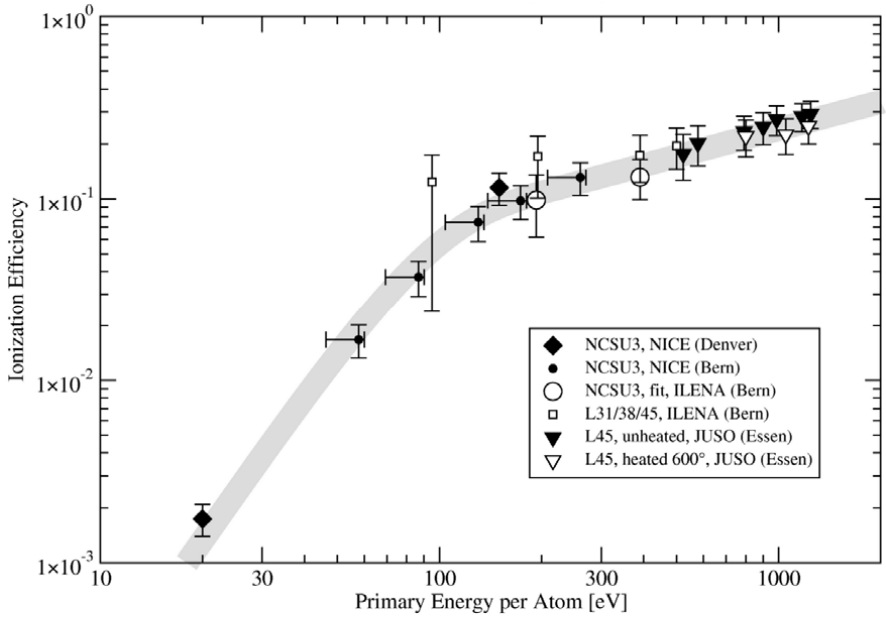

FIG. 4: Efficiency for creating negative oxygen ions upon scattering from several synthetic diamond coatings on silicon [14]. Measurements have been performed at different laboratories with different experimental setups.

measurements using the IBEX prototype at the calibration facility of the University of Bern [14]. For the diamond coatings several samples were used and the results agree, demonstrating the reproducibility of the diamond coating for our purposes. For MgO earlier data at higher energies were reported [35], which were found to agree well with our data and are shown in Fig. 5.

All these ionisation yields, $\eta^-(E)$, can be fitted by the following, experimentally found, function using the experimental data from Figs. 3 to 5:

$$\eta^-(E) = \eta_0^- \left\{ 1 - \exp\left(- \left(\frac{E}{E_0} \right)^b \right) \right\} \left(\frac{E}{E_0} \right)^a , \qquad (4)$$

where E_0 is the roll over energy, η_0^- is a scaling factor, and a and b are experimental constants. The individual parameters derived from the data presented in Figs. 3 to 5 are listed in Table I. The exponent a gives the fall off at low energies, which is 1.5 and 2.44 for H and O on the diamond coatings, respectively. The roll over is at an energy of $E_0 \approx 20$ eV for H (not that well constrained by our data) and at $E_0 \approx 118$ eV for O and on the diamond coatings, and at $E_0 \approx 108$ eV for O on the MgO surface. These roll over energies suggest a common roll over velocity of $v_C \approx 4 \times 10^4$ m/s for the three data sets (Figs. 3 to 5) and we can rewrite Eq. (4) as

$$\eta^-(v) = \eta_0^- \left\{ 1 - \exp\left(- \left(\frac{v}{v_C} \right)^{2b} \right) \right\} \left(\frac{v}{v_C} \right)^{2a} \qquad (5)$$

The exponent b gives the yield dependence at energies above the roll over that is compatible with an $\eta^- \propto v$ dependence, which is similar to KEE at higher energies.

IV. DISCUSSION

Detection of ENAs using KEE is a simple method. The advantage of using KEE for the detection of ENAs is that it allows for a very compact realisation of an instrument, which is a major asset in space research. The NPD sensor, for example, weights only 720 g complete with sensor electronics. The ASPERA-3 instrument with the NPD sensor is in operation since December 2003 in Mars orbit and is still taking measurements. The ASPERA-4 instrument, an almost identical copy of this instrument, is on the Venus Express mission, which was launched 9 November 2005. If transfer to Venus is successful it will commence scientific measurements in April 2006. The disadvantage of this simple time-of-flight measurement is the limited velocity resolution, since the energy scattering and the angle scattering at the start surface combine to limit the time-of-flight resolution of the instrument to about 30% in a space compatible configuration [5]. Moreover, the mass resolution hinges on the different secondary electron yields for different species arriving at the same velocity, which allows only for a coarse mass identification. If one needs better-resolved measurements it is necessary to ionise the ENAs before their analysis. The limitation of neutral particle detection via KEE is the low KEE yield at low particle energies, which limits the useful energy range to 100 eV and above. Since the ENA is not ionised only moderate analysis of the registered ENAs can be performed.

Using the surface ionisation technique a full analysis of the ENA is possible and the useable energy range extends down to about 10 eV. The limitation in energy arises from sputtering of negative ions by higher energy ENAs, which cannot be hindered to reach the conversion surface in a space borne application. Since a truly ionised 10 eV ENA cannot be distinguished from a negative ion sputtered by a

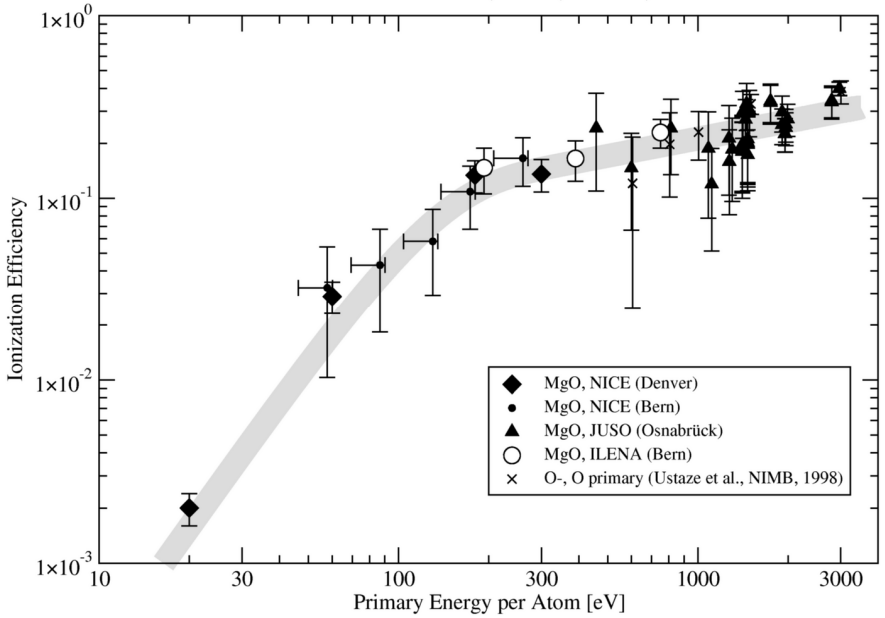

FIG. 5: Efficiency for creating negative oxygen ions upon scattering from the (100) surface of MgO single crystals [14, 35]. Measurements have been performed at different laboratories with different experimental setups.

higher energy primary particle one has to disregard these low-energy ions. Other ionisation techniques, like electron impact ionisation may be used at energies below 10 eV.

The newest and most sensitive instruments using surface ionisation were developed for the detection of the interstellar gas, first the NICE instrument prototype [22] and recently the IBEX-Lo instrument prototype [14]. Both of these instruments use artificial diamond surfaces to ionise incoming neutral atoms. The latter instrument is part of the scientific payload of the IBEX mission of NASA to be launched in June 2008 to study the interaction of solar wind plasma with the interstellar medium [40].

The physical mechanism of negative ion formation on metal surfaces is well understood, and mainly governed by the work function of the surface and the affinity level of the atom [25]. The exact physical mechanism of negative ion formation on insulating surfaces is much less known [41]. Detailed experimental and theoretical studies are available for hydrogen and fluorine atoms scattering off LiF, an ionic crystal [42, 43]. However if these mechanisms also operate on diamond, which is a covalent crystal, as scattering surface has still to be seen. Our experimental experience is that surfaces that have high KEE yields also work well for surface ionisation. This implies that the localised electronic excitation near the surface during particle impact (the electronic energy loss), which gives rise the KEE also facilitates the electron transfer to the projectile. It would be interesting to understand the exact mechanism for at least two reasons. Firstly, because of pure scientific interest, and secondly because a good understanding of the underlying physics will allow us for a much more directed search for the perfect surface for ionisation.

Acknowledgments

The collaboration with S. Fuselier and E. Hertzberg, Lockheed Martin Advanced Technology Center, CA, USA, and W. Heiland, University of Osnabrück, Germany, is gratefully acknowledged. This work is supported by Swiss National Science Foundation.

[1] P. Wurz, in: *The Outer Heliosphere: Beyond the Planets*, Eds. K. Scherer, H. Fichtner, E. Marsch,(Copernicus Gesellschaft e.V., Katlenburg-Lindau, Germany, 2000).
[2] P. Wurz, M. R. Aellig, P. Bochsler, A. G. Ghielmetti, E. G. Shelley, S. A. Fuselier, F. Herrero, M. F. Smith, T. S. Stephen, Opt. Eng. **34**, 2365-2376 (1995).
[3] T. E. Moore, *et al.*, Space. Sci. Rev. **91**, 155-195 (2000).
[4] J. Burch, Space Sci. Rev. **91**, 1-14 (2000).
[5] S. Barabash, *et al.*, ESA-SP **1240**, 121-139 (2004).
[6] S. Barabash, *et al.*, Planet. Space Science, submitted (2005).
[7] A. Bhardwaj, S. Barabash, Y. Futaana, Y. Kazama, K. Asamura, R. Sridharan, M. Holmström, P. Wurz, R. Lundin, Jou. Earth System Science, in press (2005).
[8] A. Milillo, *et al.*, Space Sci. Rev. **117**, 397- (2005).
[9] M. Wieser, P. Wurz, R. J. Nemanich, S. Fuselier, Jou. Appl. Phys. **98**, 1-4 (2005).
[10] S. M. Ritzau, R. A. Baragiola, Phys. Rev. B **58**, 2529-2538 (1998).
[11] G. Betz, K. Wien, Int. J. Mass Spectr. **140**, 1-110 (1994).
[12] J. Cazeaux, in: *Ionization of Solids by Heavy Particles*, Ed. R. A. Baragiola, (Plenum Press, New York, 1993).
[13] S. A. Deutscher, A. Borisov, V. Sidis, Phys. Rev. A **59**, 4446-4455 (1999).
[14] M. Wieser, *Detection of energetic neutral atoms and its application to heliospheric science*, Bern, University of

Bern, 2005, p. 221.
[15] S. Jans, *Definition of the optical components for the NPD sensor on Mars Express*, University of Bern, Switzerland, 2000.
[16] J. Yarmoff, T. Lui, S. Qiu, Z. Sroubek, Phys. Rev. Lett. **80**, 2469-2472 (1998).
[17] H. Eder, F. Aumayr, H. Winter, Nucl. Instr. Meth. B **154**, 185-193 (1999).
[18] J. Lörincík, Z. Sroubek, H. Eder, F. Aumayr, H. Winter, Phys. Rev. C **62**, 16116-16125 (1999).
[19] J. Lörincík, Z. Sroubek, S. Cernusca, A. Diem, H. Winter, Surf. Sci. **504**, 59-65 (2002).
[20] P. Wurz, P. Bochsler, A. G. Ghielmetti, E. G. Shelley, F. Herrero, M. F. Smith, *Concept for the HI-LITE Neutral Atom Imaging Instrument*, Kaprun, Austria, 1993, pp. 225230.
[21] H. Hotop, W. C. Lineberger, J. Phys. Chem. Ref. Data **14**, 731-750 (1985).
[22] M. Wieser, P. Wurz, P. Bochsler, E. Moebius, J. Quinn, S. Fuselier, A. Ghielmetti, J. DeFazio, T. M. Stephen, R. J. Nemanich, Meas. Sci. Technol. **16**, 1667-1676 (2005).
[23] J. N. M. van Wunnik, J. J. C. Geerlings, E. H. A. Granneman, J. Los, Surf. Sci. **131**, 17 (1983).
[24] J. J. C. Geerlings, P. W. vanAmersfoort, L. F. T. Kwakman, E. H. A. Granneman, J. Los, J. P. Gauyacq, Surf. Sci. **157**, 152-161 (1985).
[25] J. Los, J. J. C. Geerlings, Phys. Reports **190**, 133-190 (1990).
[26] N. D. Lang, Phys. Rev. B **4**, 4234-4244 (1971).
[27] C. F. A. van Os, P. W. Amersfoort, J. Los, J. Appl. Phys. **64**, 3863-3873 (1988).
[28] R. Schletti, T. Fröhlich, P. Wurz, Rev. Sci. Instr. **71**, 499-503 (2000).
[29] A. G. Ghielmetti, E. G. Shelley, S. Fuselier, P. Wurz, P. Bochsler, F. Herrero, M. F. Smith, T. Stephen, Opt. Eng. **33**, 362-370 (1994).
[30] P. Wurz, R. Schletti, M. R. Aellig, Surf. Sci. **373**, 56-66 (1997).
[31] P. Wurz, T. Fröhlich, K. Brüning, J. Scheer, W. Heiland, E. Hertzberg, S. A. Fuselier, *Formation of Negative Ions by Scattering from a Diamond(111) Surface*, Prague, Czech Republic, Charles University, 1998, pp. 257-262.
[32] J. A. Scheer, M. Wieser, P. Wurz, P. Bochsler, E. Hertzberg, S. Fuselier, R. J. Nemanich, M. Schleberger, Nucl. Instr. Meth. B **230**, 330-339 (2005).
[33] S. Jans, P. Wurz, R. Schletti, T. Fröhlich, E. Hertzberg, S. A. Fuselier, J. Appl. Phys. **85**, 2587-2592 (2000).
[34] S. Jans, P. Wurz, R. Schletti, K. Brünning, K. Sekar, W. Heiland, J. Quinn, R. E. Leuchtner, Nucl. Instr. B **173**, 503-515 (2001).
[35] S. Ustaze, R. Verucchi, S. Lacombe, L. Guillemot, V. A. Esaulov, Phys. Rev. Lett. **79**, 3525-3529 (1997).
[36] M. Wieser, P. Wurz, K. Brüning, W. Heiland, Nucl. Instr. Meth. B, in press (2002).
[37] C. Auth, A.G. Borisov, H. Winter, Phys. Rev. Lett. **75**, 2292-2295 (1995).
[38] J. A. Scheer, P. Wurz, W. Heiland, Nucl. Instr. Meth. B **212**, 291-296 (2003).
[39] B. Willerding, H. Steininger, K. J. Snowdon, W. Heiland, Nucl. Instr. Meth. B **2**, 453-456 (1984).
[40] D. McComas, *et al.*, AIP Conference Proceedings **719**, 162-181 (2004).
[41] A. G. Borisov, V. A. Esaulov, J. Phys.: Condens. Matter **12**, R177-R206 (2000).
[42] H. Winter, Prog. Surf. Sci. **63**, 177-247 (2000).
[43] H. Winter, Nucl. Instr. Meth. B **212**, 45-50 (2003).